

Simulation of Fracturing Reinforced Polymer Blends

Galen T. Pickett,¹ David Jasnow,² and Anna C. Balazs¹

¹Materials Science and Engineering Department, University of Pittsburgh, Pittsburgh, Pennsylvania 15261

²Department of Physics and Astronomy, University of Pittsburgh, Pittsburgh, Pennsylvania 15261

(Received 18 January 1996)

Brownian dynamics simulations are used to simulate the fracture of a polymer/polymer interface that is reinforced by “connector” chains. The connectors can weave back and forth across this boundary, forming either single or multiple “stitches.” The work needed to fracture this interface is calculated as a function of the architecture and conformation of the connectors. The results show that the multistitch connectors dramatically improve the strength of the interface. This is rationalized through scaling arguments and explains recent experimental studies. The conclusions provide experimental guidelines for synthesizing effective connectors and thereby fabricating high-strength composites. [S0031-9007(96)00732-6]

PACS numbers: 62.20.Mk, 81.05.Qk

The process of alloying or blending existing polymers holds considerable promise as a means of creating new materials at a relatively low cost. Most polymer pairs, however, are immiscible, and the mixture segregates into macroscopic domains, separated by relatively sharp, weak interfaces. Consequently, the bulk material exhibits poor mechanical properties. A key to forming high-strength blends [1] is to “compatibilize” the mixture, i.e., create a fine dispersion of small domains. A second key is to toughen or strengthen the interfaces. A small amount of a third polymer can act as both a compatibilizer [2] and a toughening agent [3,4]. In blending polymers *A* and *B*, the additive is typically a copolymer composed of both *A* and *B* monomers. *AB* diblock copolymers contain a long block of *A* units chemically linked to a long block of *B*'s; random copolymers contain a random arrangement of *A* and *B* monomers along the length of the chain. While diblock copolymers are more efficient compatibilizers than random copolymers [5], there is evidence that random copolymers are more effective as toughening agents. In experiments on reinforcing the interface between polystyrene (PS) and polyvinylpyridine (PVP) at equal numbers of chains per unit area, random PS-PVP copolymers yield a significantly higher fracture toughness, and thus a stronger interface, than diblocks [4]. As random copolymers are far less expensive than highly regular copolymers like diblocks, demonstrating the generality of this observation would have important implications for producing low-cost, high-strength blends.

Both diblock and random copolymers can cross and entangle with the two homopolymers separated by an interface. This behavior enhances the adhesion and, thereby, improves the mechanical integrity of the blend. The equilibrium conformations of these copolymers at the interface are, however, quite different. A random copolymer can loop back and forth across the *A/B* boundary [6], forming multiple “stitches” [see Fig. 1(a)]

[7]. In contrast, a diblock forms a single stitch [8]: the *A* block extends into the *A* domain, and the *B* block is localized in the *B* region [see Fig. 1(b)]. The ability of random copolymers to form many stitches is thought to be the key to their toughening behavior [4,6].

In the Letter, we use computer simulations to quantify the effect of “multistitching” on the interfacial strength. While equilibrium theories can reveal the conformation of the copolymer at the *A/B* boundary, they are not able to account for the unique toughening attributes of random copolymers [5,9]. Here, we use a Brownian dynamics simulation to model the fracture of an *A/B* interface that is stitched by a “connector” chain. Using the dynamical model, we calculate the work necessary to fracture the interface as a function of the number of stitches, and therefore correlate interfacial strength with the architecture of the copolymer additive.

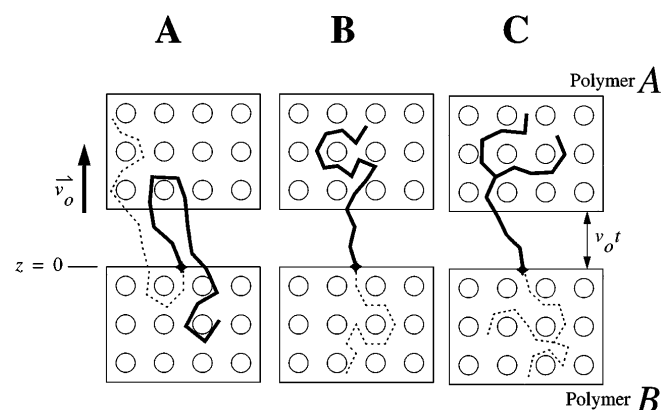


FIG. 1. Schematic of the simulation. The incompatible polymer matrices are modeled as rigid arrays of obstacles. Here, (a) shows the typical interfacial conformation of a random copolymer, (b) represents a diblock, and (c) indicates the T-shaped chain. The dashed lines represent other portions of the chains, for example, the *B* block of the diblock, which we do not treat. The upper *A* phase is in constant motion with $v_0 = k_B T (\nu D)^{-1}$.

Under deformation, the interface can fail through three mechanisms [10]. First, if the stress along the backbone of the connector becomes too large, it can break. Second, the connectors can be pulled out of the entangling homopolymer matrix. Third, if sufficient stress is transferred to the matrix, the bulk material can fail by forming fibrils or crazes. In this study, we focus on chain pullout. This mechanism enables chains grafted to a surface to act as a lubricating layer [11] or decrease the slippage of a flowing polymer melt [12]; thus, disentangling of chains under mechanical deformation is an important phenomenon not only in this, but also other problems relevant to the processing of polymer materials.

In our simulation, the polymer matrix is modeled as a two-dimensional array of fixed obstacles [13], as shown in Fig. 1. The obstacles provide lateral constraints on the motion of the connectors, defining the walls of an effective “tube” [14]. This tube can wrap around, but not cross, the obstacles. The connector consists of N beads joined by rigid links of length l . Each bead in this freely jointed chain is subjected to forces arising from the surrounding matrix; the Langevin equation of motion for bead i at \mathbf{r}_i is

$$\begin{aligned} d\mathbf{r}_1/dt &= 0, \\ \nu(d\mathbf{r}_i/dt - \mathbf{v}_m) &= \mathbf{T}_{i-1} + \mathbf{T}_i + \mathbf{F}_i + \mathbf{f}_i, \\ &\text{for } 2 < i < N, \\ \nu(d\mathbf{r}_N/dt - \mathbf{v}_m) &= \mathbf{T}_{N-1} + \mathbf{F}_N + \mathbf{f}_N. \end{aligned} \quad (1)$$

Here, ν is the effective viscous damping per bead, and \mathbf{v}_m is the velocity of the surrounding matrix; it vanishes for the lower matrix and is a constant in the upper matrix. The force \mathbf{T}_i is the tension in the link connecting the i th and $(i + 1)$ th beads. The \mathbf{T}_i 's are determined self-consistently by instantaneously applying the constraints

$$\begin{aligned} d|\mathbf{r}_{i+1} - \mathbf{r}_i|^2/dt &= 0, \\ &\text{for } 1 < i < N - 1, \end{aligned} \quad (2)$$

which ensure that the links are of constant length. The first bead is permanently grafted to the upper surface of the lower matrix, and hence is stationary. The last bead is only affected by the tension in the final link and friction. \mathbf{F}_i is a short-range repulsive force between obstacles and the i th bead and is given by [15]

$$\mathbf{F}_i = \mathbf{F}(\Delta\mathbf{r}_i) = \begin{cases} \sigma\Delta\mathbf{r}_i[4/(4\Delta r_i^2 - l^2) - 4/3l^2]^2, & \text{for } l/2 < |\Delta\mathbf{r}_i| < l, \\ 0, & \text{for } l < |\Delta\mathbf{r}_i|, \end{cases} \quad (3)$$

where $\Delta\mathbf{r}_i$ is the displacement from the nearest obstacle to the i th bead. Such a force field will prevent a rod of length l from crossing through the hard core of an obstacle (at $l/2$), so that a chain of many links may loop around but never cross it. The temperature of the matrix is conveyed to the connector via the Gaussian noise \mathbf{f}_i , with correlator $\langle f_i(t) f_j(t') \rangle = 2\nu k_B T \delta_{ij} \delta(t - t')$. Here, k_B is Boltzmann's constant and T is temperature. This part of the algorithm is adapted from a model of DNA in gel electrophoresis [15].

We choose the distance between obstacle centers, D , so that $D = 2.5l$. This fact and the soft core of the potential in Eq. (3) ensures that the matrix has sufficient free area (comparable to free volume in 3D) for the connectors to readily move about the lattice. This free area means that our simulation models an elastomeric material, rather than a glass. Additionally, we interpret D as the length of an elementary “step” within the tube.

The upper matrix ($z > 0$) is labeled polymer A , and the lower matrix ($z \leq 0$) is composed of polymer B . We set the A matrix in an upward motion at $t = 0$ with a constant velocity, $v_0 = k_B T (\nu D)^{-1}$. We emphasize that this corresponds to a relatively fast pulling rate.

To calculate the work needed to separate the A and B matrices stitched by a connector, we determine the force transmitted to the A matrix by the connector. Let $\{n_i\}$ be the set of links at time t that cross the boundary of the A

matrix at $z = v_0 t$. Given \mathbf{z} as the upward unit vector,

$$P = v_0 \sum_i |T_{n_i} \cdot \mathbf{z}| \quad (4)$$

is the power that must be supplied to keep the upper surface moving with the velocity v_0 . (We prevent the beads in the gap from contributing to P .) The total work to separate the matrices to infinity is given by $G = \int P dt$.

In the case of single-stitch connectors (8), the chains are initially grafted to the B matrix and are prevented from re-visiting the B region. The connector adopts an otherwise random conformation. Within this regime, we probe the effect of molecular architecture by comparing linear connectors to connectors of identical molecular weight but with a T architecture [see Fig. 1(c)]. Figure 2 reveals that the branched species is slightly less efficient than the linear one, but both architectures are consistent with $G \sim N^2$ [16] over the range of accessible N [10,17]. On average, branched connectors penetrate less deeply than linear connectors, thereby forming fewer entanglements with the matrix.

In the multistitch case, the connector crosses the AB interface many times, but not all of the resulting loops “catch” on obstacles. We classify the initial configuration by the number of effective stitches it possesses. We developed an algorithm to identify the effective number of stitches. In particular, we divide the chain into loops that cross $z = 0$, and determine which of these wind

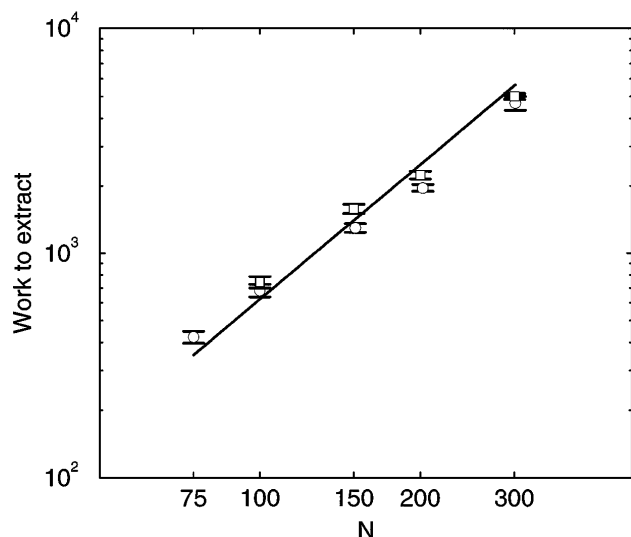


FIG. 2. Log-log plot of G vs N for linear and branched single-stitch connectors. The symbol \square indicates the linear connector and \circ represents the branched connectors. Branching of the connector does not significantly degrade its toughening ability. The data are consistent with $G \sim N^2$ (solid line) for both architectures.

around one or more obstacles. The first loop that catches on obstacles in the A matrix is the first effective loop. The next loop that catches B obstacles is the second effective loop. Continuing in this manner, we determine the number of alternating, effective loops. To determine the number of stitches s , we add 1 to this number to account for the chain's dangling tail. If there are no effective loops in the chain, and the tail extends into A , we classify that configuration as 1 stitch.

Figure 3(a) shows how G is affected by varying s and, with the understanding that the systems considered are small, Fig. 3(b) suggests that $G(N, s) \sim sN^2$. Clearly, entangling across the interface enhances the fracture energy. In a real sample, there is a distribution of the number of stitches. To determine the overall strength, we weight $G(N, s)$ by the distribution. We thereby make a direct comparison of multistitch (random) and single-stitch (diblock) copolymers in Fig. 4. We find that for $N > 100$ many stitch connectors are more effective tougheners than single-stitch connectors, and that the results for the former are consistent with $G \sim N^{2+\alpha}$ where $\alpha = 0.5$. Note that the ratio between the multistitch and single-stitch cases grows as $\sim N^{1/2}$, an appreciable quantity even for modest values of N .

One assumption we make is that the connectors do not break. To determine if this is reasonable, consider a chain of N beads that is nearly fully extended and dragged by one end at the velocity v_0 . The tension in the first link supports the motion of the entire chain: $T_{\max} = \nu v_0 N$. The chain will break if $T_{\max} \approx 50$ eV/nm [4]. Taking $l = 1$ nm and $k_B T = 1/40$ eV, we find that chain breaking is unimportant for $N < 2000$. Our simulations

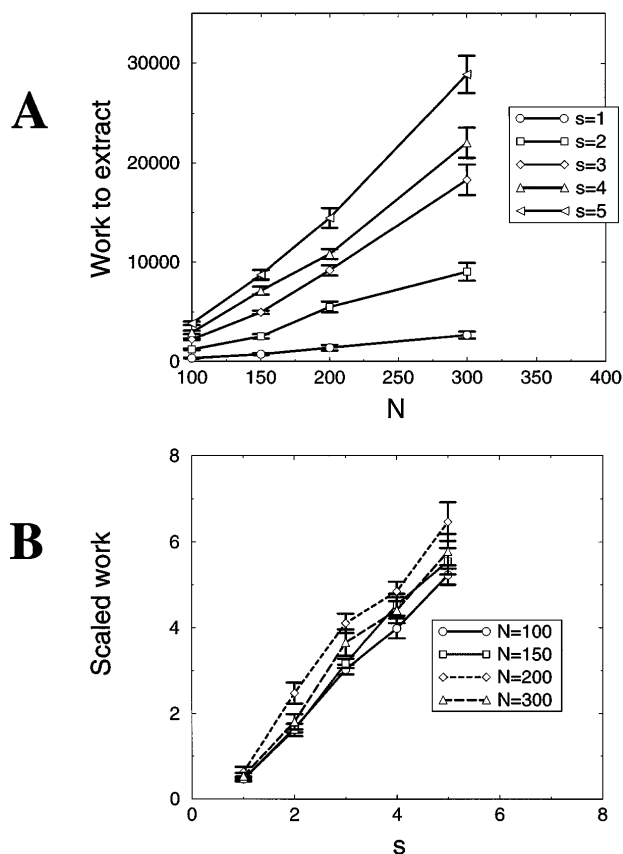


FIG. 3. (a) G vs N for a fixed number of stitches in the initial configuration. Clearly, multistitch conformations improve the interfacial strength. (b) G vs s , the number of stitches, at constant N . G has been normalized by the single-stitch value in Fig. 2. The collapse of the data indicates that $G \sim sN^2$.

are restricted to molecular weights far less than this value for computational reasons.

We rationalize our results with simple scaling arguments [18,19]. The time scale on which pullout happens is $t_p \sim Nl v_0^{-1} \sim Nl^2 \nu / k_B T$. The time required for a grafted chain to completely renew its configuration is much longer; unhindered by the obstacles, it is the Rouse relaxation time, $t_r \sim (N^2 l^2 \nu) / k_B T \sim N t_p$. With the obstacles turned on, the required time is much longer: $t \sim \exp(t_p)$ [20]. Therefore, on time scales relevant for pullout, the connector is effectively confined to a static "tube." The obstacles serve to restrict the connector's lateral movement, so that beads on the chain all move along the same path in the matrix. To estimate the work needed to pull the connector out, we imagine dragging each of the N beads along the contour of the tube. Analogous to the rope in "block and tackle" pulleys [7,19], when the gap widens by a distance dz , each of the s stitches lengthens by dz as well. Hence, the tail must supply approximately $s dz / l$ beads. Therefore, the average velocity over all the beads increases as s . Consequently, the average force that must be applied to each bead is $\sim \nu s v_0$. The contour length of the tube L is proportional to N . For

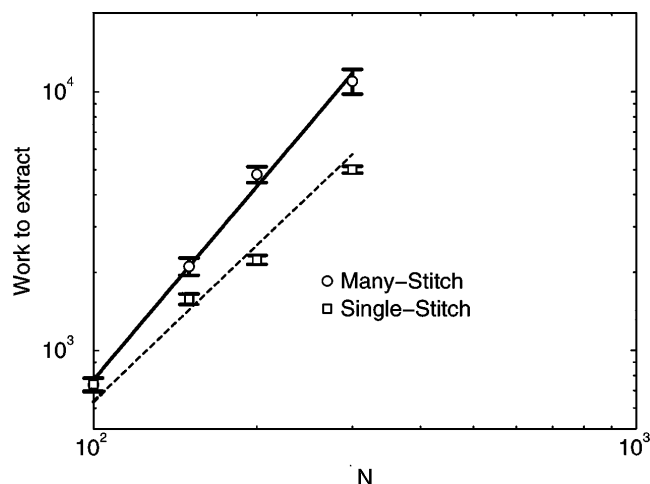


FIG. 4. G for many-stitch vs single-stitch connectors. The many-stitch data have been averaged over the possible number of stitches. The solid line has a slope of 2.5, and the dashed line has a slope of 2.0. For many-stitch connectors, $G \sim N^{2.5}$.

single-stitch connectors, we estimate that [16]

$$G \sim \nu v_0 N L \sim \nu v_0 N^2. \quad (5)$$

This scaling should hold whether or not the connector is branched. However, for many-stitch connectors,

$$G \sim \langle s \rangle_N \nu v_0 N L \sim \nu v_0 N^{(2+\alpha)}, \quad (6)$$

where the average number of stitches, $\langle s \rangle_N \sim N^\alpha$, is proportional to the number of crossings, giving $\alpha = 1/2$ for Gaussian chains.

Finally, we note that while our simulation is two dimensional, our scaling arguments are independent of dimension. Since our simulations are in agreement, we believe that our results are valid in three dimensions.

The simulations, combined with the scaling arguments, show that, at equal chains/area, many-stitch connectors are more effective at strengthening an interface than single-stitch chains. In our microscopic simulation, we are able to track the influence of specific stitching conformations, information that is all but impossible to obtain experimentally. Nonetheless, by averaging over the ensemble of stitching configurations, we offer a specific, experimentally verifiable prediction that $G \sim N^{(2+\alpha)}$, with $\alpha \cong 1/2$ for random copolymers. As random copolymers are more easily produced, our results indicate performance as well as cost advantages.

This work was funded in part by ONR Grant No. N00014-91-J-1363, NSF Grant No. DMR-9407100, and DOE Grant No. DE-FG02-90ER45438 to A.C.B.

and NSF Grant No. DMR-92-17935 to D.J. We thank Dr. D. Gersappe, Dr. C. Yeung, and Dr. M. Rubenstein for helpful discussions.

-
- [1] L. A. Utracki, *Polymer Blends and Alloys* (Hanser, New York, 1989).
 - [2] R. Israels *et al.*, *J. Chem. Phys.* **102**, 8149 (1995), and references therein.
 - [3] H. Brown, *Annu. Rev. Mater. Sci.* **21**, 463 (1991).
 - [4] C.-A. Dai *et al.*, *Phys. Rev. Lett.* **73**, 2472 (1994).
 - [5] D. Gersappe and A.C. Balazs, *Phys. Rev. E* **52**, 5061 (1995).
 - [6] C. Yeung, A.C. Balazs, and D. Jasnow, *Macromolecules* **25**, 1357 (1992).
 - [7] H. Ji and P.G. de Gennes, *Macromolecules* **26**, 520 (1993).
 - [8] E. Raphael and P.G. de Gennes, *J. Phys. Chem.* **96**, 4002 (1992).
 - [9] S. Milner and G. Fredrickson, *Macromolecules* **28**, 7953 (1995).
 - [10] J. Washiyama *et al.*, *Macromolecules* **27**, 2019 (1994); C. Creton *et al.*, *Macromolecules* **25**, 3075 (1992).
 - [11] H. Brown, *Science* **263**, 1411 (1994).
 - [12] A. Ajdari *et al.*, *Physica (Amsterdam)* **204A**, 17 (1994).
 - [13] Each obstacle represents the presence of *many* entangled chains that the connector encounters. In the fast pullout regime, the matrix is not significantly distorted during the pullout process. Thus, our model of rigid obstacles is appropriate.
 - [14] P.G. de Gennes, *Scaling Concepts in Polymer Physics* (Cornell University Press, Ithaca, 1979), Chap. 8.
 - [15] J.M. Deutsch, *Science* **240**, 922 (1988); J.M. Deutsch and T.L. Madden, *J. Chem. Phys.* **90**, 2476 (1989).
 - [16] We are able to simulate chains with N between 100 and 300, less than half a decade in molecular weight. Thus, the exact slope of the data in Fig. 2 is less important than the qualitative support it lends to our scaling arguments. For small N , the tube picture breaks down, and we expect that $G \sim N$, since N beads get pulled out. It is possible that the crossover from $G \sim N$ to $G \sim N^2$ affects the apparent exponent in Figs. 2 and 4 for single-stitch chains.
 - [17] B. Lin and P.L. Taylor, *Macromolecules* **27**, 4212 (1994).
 - [18] M. Rubenstein, L. Leibler, and A. Ajdari, *Polym. Preprints* **53**, 628 (1994); K.P. O'Connor and T.C.B. McLeish, *Polymer* **33**, 4314 (1992); K.E. Evans, *J. Polym. Sci.* **25**, 353 (1987); P. Prentice, *Polymer* **24**, 346 (1983).
 - [19] T.C.B. McLeish, C.J.G. Plummer, and A.M. Donald, *Polymer* **30**, 1651 (1989).
 - [20] M. Doi and S.F. Edwards, *The Theory of Polymer Dynamics* (Clarendon Press, Oxford, 1986).